β-Amyloid precursor protein transgenic mice that harbor diffuse Aβ deposits but do not form plaques show increased ischemic vulnerability: Role of inflammation

Milla Koistinaho*, Mikko I. Kettunen*, Gundars Goldsteins*, Riitta Keinänen*, Antero Salminen†, Michael Ort‡§, Jan Bures‡, David Liu¶, Risto A. Kauppinen*, Linda S. Higgins¶, and Jari Koistinaho*‖**

*A.I. Virtanen Institute for Molecular Sciences, †Department of Neurology and Neuroscience, ‖Department of Clinical Pathology of Kuopio University Hospital, University of Kuopio, P.O. Box 1627, FIN-70211, Kuopio, Finland; ‡Institute of Physiology, Academy of Sciences of the Czech Republic, Videnska 1083, 142 20 Prague 4-Krc, Czech Republic; §Department of Psychiatry, First School of Medicine, Charles University, Ke Karlovu 11, 128 08 Prague 2, Czech Republic; and ¶Scios Incorporated, Sunnyvale, CA 94085

Contributed by Jan Bures, December 14, 2001

β-amyloid (Aβ), derived form the β-amyloid precursor protein (APP), is important for the pathogenesis of Alzheimer's disease (AD), which is characterized by progressive decline of cognitive functions, formation of Aβ plaques and neurofibrillary tangles, and loss of neurons. However, introducing a human wild-type or mutant APP gene to rodent models of AD does not result in clear neurodegeneration, suggesting that contributory factors lowering the threshold of neuronal death may be present in AD. Because brain ischemia has recently been recognized to contribute to the pathogenesis of AD, we studied the effect of focal brain ischemia in 8- and 20-month-old mice overexpressing the 751-amino acid isoform of human APP. We found that APP751 mice have higher activity of p38 mitogen-activated protein kinase (p38 MAPK) in microglia, the main immune effector cells within the brain, and increased vulnerability to brain ischemia when compared with age-matched wild-type mice. These characteristics are associated with enhanced microglial activation and inflammation but not with altered regulation of cerebral blood flow, as assessed by MRI and laser Doppler flowmetry. Suppression of inflammation with aspirin or inhibition of p38 MAPK with a selective inhibitor, SD-282, abolishes the increased neuronal vulnerability in APP751 transgenic mice. SD-282 also suppresses the expression of inducible nitric-oxide synthase and the binding activity of activator protein 1. These findings elucidate molecular mechanisms of neuronal injury in AD and suggest that antiinflammatory compounds preventing activation of p38 MAPK in microglia may reduce neuronal vulnerability in AD.

The β-amyloid precursor protein (APP) is a ubiquitous transmembrane glycoprotein and the source of β-amyloid peptides (Aβ), which are the principal components of amyloid plaques in the brain of patients with Alzheimer's disease (AD), an age-related neurodegenerative disease associated with progressive decline of cognitive functions (1, 2). Other hallmarks of AD include the formation of neurofibrillary tangles in neurons, loss of synapses, and decreases in cell density in the distinct regions of the brain. These histopathological changes are observed in familial AD, which is caused by mutations in the APP or presenilin genes, in sporadic AD, and in individuals with Down's syndrome, who carry an extra copy of chromosome 21 and overexpress wild-type APP several fold in the brain (3–6).

Substantial evidence indicates importance of APP for the pathogenesis of AD, but the mechanism how APP increases neuronal vulnerability in AD is unclear. A large number of epidemiological studies indicate that inflammatory events are involved because antiinflammatory drugs slow the progression of the disease, and reactive microglia and proinflammatory molecules that are secreted by microglia are present at sites of amyloid plaques (7–11). The inflammation hypothesis is further supported by the findings that secreted derivatives of APP (sAPP-α) and Aβ activate microglial cells resulting in death of primary neurons *in vitro* (12–14). However, correlation of amyloid with neuronal death in AD patients is controversial (15), and several mouse lines transgenic (TG) for wild-type or mutant APP or mutant presenilin genes develop amyloid deposits and chronic inflammation in the brain without increased neuronal loss (16–19), suggesting that additional contributory factors that lower the threshold of neuronal death may be present in AD.

There is ample evidence that ischemic stroke, another dementia-causing disease in the elderly, may contribute to the pathogenesis of AD. First, epidemiological studies suggest that risk factors for stroke are associated with AD (reviewed in ref. 20). Second, 60–90% of AD patients show cerebrovascular pathology at autopsy, and coexistence of stroke and AD occurs more than by chance alone (21). Third, stroke intensifies the presence and severity of the clinical symptoms of AD and increases AD pathology in the brain (22, 23). However, the molecular mechanism how ischemia may be associated with AD is unclear.

Because proinflammatory pathways are triggered both in stroke (24–27) and AD (10, 11), and antiinflammatory compounds are beneficial in animal models of these diseases (25, 28–32), we hypothesized that pathological metabolism of APP enhances inflammation, thereby sensitizing the brain to ischemic insults. To test this hypothesis, we used 8- and 20-month-old mice overexpressing human wild-type APP751 in neurons at the level comparable to APP expression in individuals with Down's syndrome (33). These mice develop diffuse Aβ deposition and show age-related, specific learning deficits that are independent of amyloid plaque formation (34–36). We report that the brains of these mice have increased activity of microglial p38 mitogen-activated protein kinase (p38 MAPK), a central mediator of inflammation, and increased ischemic vulnerability, which is not because of altered regulation of cerebral blood flow but is associated with enhanced inflammation. We also show that inhibition of inflammation by aspirin or inhibition of p38 MAPK by a selective inhibitor abolishes the increased inflammation and sensitivity of the TG mouse brain to ischemia. Thus, neuronal expression of APP may sensitize AD brain to ischemic and

Abbreviations: Aβ, β-amyloid peptide; AD, Alzheimer's disease; AP-1, activator protein 1; APP, β-amyloid precursor protein; CBF, cerebral blood flow; iNOS, inducible nitric-oxide synthase; MAPK, mitogen-activated protein kinase; MAPKAP kinase-2, MAPK-activated protein kinase 2; MCA, middle cerebral artery; sAPP-α, secreted APP; TG, transgenic; WT, wild type; RT, reverse transcriptase.

**To whom reprint requests should be addressed. E-mail: jari.koistinaho@uku.fi.

The publication costs of this article were defrayed in part by page charge payment. This article must therefore be hereby marked "*advertisement*" in accordance with 18 U.S.C. §1734 solely to indicate this fact.

inflammation-mediated brain injuries, most likely by mechanisms independent of fibrillar Aβ accumulation.

Methods

Animals. All mouse studies were approved by the Animal Care and Use Committee of Kuopio University and follow the National Institutes of Health guidelines for animal care. Mice carrying human wild-type APP751 cDNA under the control of rat neuron-specific enolase promoter have been described (33). Male, homozygous TG mice originating from two different founder mice (F10 and F15) were used. Both TG pedigrees express 2- to 3-fold the amount of human APP751 protein compared with endogenous mouse APP levels. JU mice of the parental inbred strain served as wild-type (WT) controls. The 8-month-old cohorts were characterized behaviorally at 6 months of age (34).

Induction of Focal Cerebral Ischemia. Mice were anesthetized with 5% halothane (70% N_2O/30% O_2) for induction and 1% halothane for maintenance. The rectal temperature was maintained at 36–37°C with a heating pad. Middle cerebral artery (MCA) was exposed (37) and occluded permanently by electrocoagulation.

Drug Treatments. Aspirin (ASA, Sigma) was administered to 8-month-old APP751 TG or WT mice i.p. at the dose of 20 mg/kg four times at 4-h intervals starting 4 h before the MCA occlusion; 10 mg/kg of a novel p38 MAPK inhibitor (Scios, Sunnyvale, CA), SD-282, was administered i.p. to 8-month-old mice at 2 h before, 0, 4, and 8 h after the MCA occlusion. Vehicle control mice of the same age were injected with comparable volumes of diluent (0.5% Tween 20 in saline for SD-282, EtOH in saline for ASA).

MRI. A 4.7 T horizontal magnet (Magnex Scientific, Abdington, UK) equipped with actively shielded field gradients (Magnex Scientific) interfaced to a SMIS console (Guildford, UK) was used. T_2-weighted multislice images (TR 2100 ms, TE 55 ms, matrix size 256 $\times$ 128, 20-mm field of view, 0.6-mm slice thickness, 25 slices, a single-spin echo method) were used for the determination of the infarct volume from the anesthetized mice 24 h after the MCA occlusion. Results (mean $\pm$ SEM) are expressed as lesion volume percentage from the volume of the contralateral hemisphere. Differences among means are compared with ANOVA followed by Newman–Keuls post hoc test.

A bolus tracking method was used for perfusion MRI to assess the cerebral hemodynamic status. Twenty-four hours before and after the MCA occlusion, 80 μl of gadodiamide (0.5 mmol/liter, Omniscan, Nycomed, Oslo) was rapidly injected into a femoral vein in halothane-anesthetized mice during uninterrupted MRI data acquisition [A FLASH method, TR = 0.3 s, TE = 2.3 ms, ST = 1.5 mm, field of view = 25 mm, matrix size = 128 $\times$ 32 (zero-filled to 128 $\times$ 128 before Fourier transformation), 75 images at 0.3-s intervals]. Signal intensity variations during the transit of gadodiamide bolus were obtained and were transformed into plots of apparent $\Delta R_2^* = -\ln(S_0/S)/TE$ as a function of time. Numerical fitting of the ΔR_2^* curve into a gamma variate function was used to reduce the effects of recirculation of the contrast agent and to yield quantitative estimates of hemodynamic parameters. An apparent cerebral blood volume and mean transit time were computed from the data. The ratio of cerebral blood volume/mean transit time was used as an index of relative cerebral blood flow (relCBF) between ipsilateral and contralateral hemispheres.

Determination of Cerebral Blood Flow (CBF) and Cerebrovascular Reactivity by Laser Doppler Flowmetry. A laser Doppler probe (OxyFlo, Oxford Optronix, Oxford, UK) was placed in the center (1 mm caudal to bregma, 3.5 mm lateral to the midline) and the periphery of the ischemic territory (4.5 mm caudal to bregma, 3 mm lateral to the midline). CBF was monitored continuously 10 min before and 20 min after the MCA occlusion, and data were analyzed with PowerLab System software (A. D. Instruments, Castle Hill, Australia). The procedure for testing microvascular reactivity in mice was modified from Zhang *et al.* (38). Briefly, a 1.5-mm hole was drilled 3 mm caudal to bregma and 2 mm lateral to the midline. The dura was removed carefully, and the cortex was superfused with Ringer's solution (pH 7.4, 37°C). CBF was monitored at the site of superfusion with a laser Doppler probe. After the CBF was stabilized, 10 μM acetylcholine (Sigma) in Ringer's solution was superfused, and CBF monitoring was continued for 5 min. Data are reported as mean $\pm$ SEM.

Physiological Parameters. A polyethylene catheter was placed into the right common carotid artery of anesthetized ischemic (24 h after the MCA occlusion) or nonischemic mice to monitor blood pressure (Cardiocap II, Datex-Ohmeda Division Instrumentarium, Helsinki, Finland) and withdraw blood. Arterial blood samples (75 μl) were analyzed for pH, partial pressure of O_2 and CO_2 using a blood gas/pH analyzer (ABL-5, Radiometer, Copenhagen). Blood glucose was determined by using a One Touch Basic analyzer (LifeScan, Mountain View, CA).

Immunohistochemistry. After perfusion with 4% paraformaldehyde, the brains were postfixed for 12 h, cryoprotected in 20% sucrose in saline for 48 h, and frozen in liquid nitrogen-cooled isopentane. Coronal sections (12 μm thick) were reacted for 48 h with a rat anti-mouse F4/80 ab (Serotec, diluted 1:50) to visualize microglial cells, rabbit anti-cow glial fibrillary acidic protein ab (Dako, diluted 1: 500), and mouse anti-neuronal nuclei ab (Chemicon, diluted 1: 1,000) and with a rabbit polyclonal phospho-p38 MAPK (Thr-180/Tyr-182) ab (New England Biolabs, diluted 1:1,000) to detect activated p38 MAPK. After incubation with biotinylated secondary ab (anti-rabbit IgG or anti-mouse IgG, Vector Elite kit, Vector Laboratories, or anti-rat IgG, Santa Cruz Biotechnology) and avidin–biotin complex (Vectastain Elite kit, Vector Laboratories), the avidin–biotin complex was visualized by H_2O_2 and diaminobenzidine or Ni-diaminobenzidine. Cell counts are expressed as mean $\pm$ SEM per field.

MAPK-Activated Protein Kinase-2 Activity Assay. p38 MAPK activity was determined indirectly from snap-frozen cortices by measuring the activity of MAPK activated protein kinase 2 (MAPKAP kinase-2), a specific substrate of p38 MAPK, with an immunoprecipitation kinase assay (Upstate Biotechnology, Lake Placid, NY) according to the manufacturer's instructions. After scanning the ECL Plus (Amersham Pharmacia) stained blots on a STORM fluoroimager (Molecular Dynamics), the detected bands were quantified by using IMAGE QUANT software (Molecular Dynamics).

Reverse Transcriptase (RT)-PCR. One microgram of DNase-treated (RQ1 DNase, RNase-free, Promega) total RNA, isolated from cortices of the mice with a 12-h MCA occlusion, served as a template in each RT-PCR (Robust RT-PCR kit, Finnzymes, Helsinki) reaction. To detect the extent of inducible nitric-oxide synthase (iNOS) mRNA expression, the specific primers were 5′-ACAACGTGAAGAAAACCCCTTGTG-3′ and 5′-ACAGTTCCGAGCGTCAAAGACC-3′ (261–284 and 796–817 in NM 010927, respectively). Reverse transcription was done at 60°C for 30 min. For PCR, the initial denaturation was done at 94°C for 2 min. Five cycles consisting of denaturation (94°C, 15 s), annealing (68°C, 30 s), and polymerization (72°C, 20 s) and another 35 cycles using an annealing temperature of 64°C were

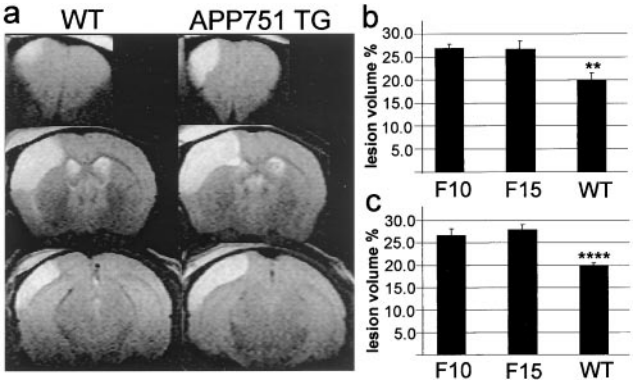

Fig. 1. MRI data reveal significantly larger lesions in APP751-overexpressing mice than in their WT littermates at 24 h after the MCA occlusion. (*a*) Typical examples of ischemic lesions in 8-month-old WT and APP751 TG mice. (*b*) At 8 months of age, both TG pedigrees develop 34% larger infarcts than WT mice (**, $P < 0.01$ from F10 and F15, ANOVA). (*c*) At 20 months, the infarcts are 35% larger in F10 pedigree and 41% larger in F15 pedigree than in WT littermates (****, $P < 0.0001$ from F10 and F15, ANOVA). $n = 6–8$ mice per group at both ages.

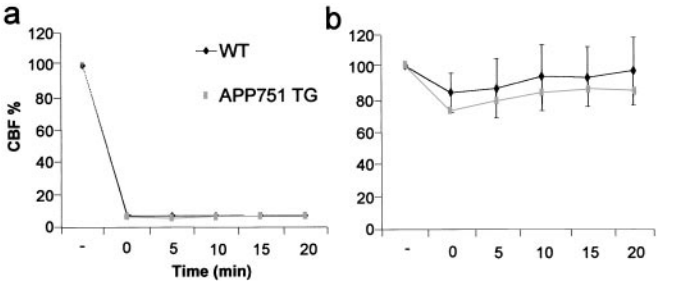

Fig. 2. Changes in CBF in response to MCA occlusion as a function of time in 8-month-old APP751 TG and WT mice. The reduction in CBF in the ischemic core (*a*) and the periphery of the ischemic territory (*b*) is similar in all time points in APP751 TG and WT mice ($P > 0.05$, *t* test, $n = 5–6$ per group). Flow before the MCA occlusion has been set to 100%.

carried out. The reaction was stopped with polymerization at 72°C for 15 min. As a reference for the iNOS expression, RT-PCR of glyceraldehyde-3-phosphate dehydrogenase was done from each sample. The specific primers were 5′-ACCACAGTCCATGCCATCAC-3′ and 5′-TCCACCACCCT-GTTGCTGTA-3′ (566–585 and 998–1,017 in NM 008084, respectively). The RT-PCR profile was as follows: reverse transcription at 50°C for 30 min, initial denaturation at 94°C for 2 min, then altogether 25 cycles composed of denaturation (94°C, 15 s), annealing (58°C, 30 s), and polymerization (72°C, 45 s), and finally the extended polymerization at 72°C for 15 min. The amplification products were analyzed by running 9-μl samples from iNOS reaction and 5-μl samples from glyceraldehyde-3-phosphate dehydrogenase reactions on a 1.8% agarose gel.

Electrophoretic Mobility-Shift Assay. To characterize the binding activity of activator protein 1 (AP-1) transcription factor in nuclear extracts, samples were prepared from cortices dissected out 2 h after the MCA occlusion by the modified method of Dignam *et al.* (39), described by Helenius *et al.* (40) in more detail. electrophoretic mobility-shift assay was performed as described earlier (40). The films were quantified by using scanned images with IMAGE QUANT software (Molecular Dynamics).

Results

APP751 TG Mice Have Increased Sensitivity to Brain Ischemia. Twenty-four hours after ischemia, a time-point where the maximal injury occurs in this model, the MRI data showed that at 8 months both TG pedigrees had 34% larger infarcts than WT mice, and at 20 months of age, the infarcts were 35% larger in the F10 pedigree and 41% larger in the F15 pedigree compared with age-matched WT mice (Fig. 1). The physiological variables were within normal range in every animal group before the MCA occlusion (data not shown) and after the MCA occlusion (Table 1). Bolus-tracking MRI experiments revealed similar perfusion parameters in APP751 TG and WT mice before and after the MCA occlusion (relCBF in intact mice: F10 0.91 ± 0.04; F15 0.97 ± 0.06; WT 0.93 ± 0.04 and 24 h after the MCA occlusion: F10 0.25 ± 0.05; F15 0.28 ± 0.03; WT 0.33 ± 0.13, for all comparisons $P > 0.05$, ANOVA). Laser Doppler flowmetry demonstrated that CBF reductions in the core and perifocal regions were not altered in the APP751-overexpressing mice compared with WT mice (Fig. 2), indicating that the difference in the infarct size between TG and WT mice was not because of greater flow reduction in APP751 mice. When the brains were exposed to topical application of 10 μM acetylcholine, which has been reported to reveal 70% impairment in vasodilator responses in mutant APP-overexpressing mice (38), no significant difference was seen in the vasodilation response between TG and WT mice (acetylcholine-induced CBF increase: APP751 TG 11 ± 5%; WT 15 ± 6%; $P > 0.05$, *t* test; $n = 5$ per group).

Increased Microglial Activation in APP751 Mice. Using dually phosphorylated p38 MAPK ab as a marker, immunohistochemical analysis revealed sparsely distributed microglial cells with activated p38 MAPK in WT mice (20 mo: 7 ± 5; 8 mo: 5 ± 4 cells), but in TG mice about 3-fold increase in the density of phospho-p38 MAPK-positive microglial cells (Fig. 3*a*) was seen throughout the brain, including the cortex (20 mo: 21 ± 2; 8 mo: 19 ± 2 cells; $P < 0.05$ for both age groups, *t* test, $n = 3–5$ mice per group). p38 MAPK activity assayed by measuring activity of MAPKAP kinase-2 supported the finding of increased p38 MAPK in APP751 mouse brain (see Fig. 5*a*). No neurons or astrocytes with phospho-p38 MAPK immunoreactivity were seen (data not shown). Thirty minutes after ischemia, a dramatic induction of phospho-p38 MAPK-positive neurons in the ischemic territory was seen both in WT (137 ± 11 neurons; $n = 3$) and TG (120 ± 10 neurons; $n = 3$) mice with no statistical

Table 1. Physiological parameters in ischemic mice

Genotype	Treatment	Blood glucose (mmol/liter)	MABP (mm Hg)	Arterial pH	Arterial pO_2 (mm Hg)	Arterial pCO_2 (mm Hg)
WT		6.7 ± 0.4	80 ± 2	7.31 ± 0.02	95.5 ± 2.8	47.7 ± 1.3
APP751 TG		6.8 ± 0.5	83 ± 3	7.32 ± 0.02	94.9 ± 4.5	45.7 ± 2.3
WT	ASA	7.7 ± 0.9	82 ± 1	7.37 ± 0.03	99.3 ± 3.1	44.8 ± 2.5
APP751 TG	ASA	7.1 ± 0.7	81 ± 1	7.34 ± 0.03	95.0 ± 3.4	45.8 ± 2.1
WT	SD-282	7.8 ± 0.7	84 ± 1	7.32 ± 0.02	97.0 ± 2.4	47.7 ± 1.2
APP751 TG	SD-282	6.9 ± 0.5	83 ± 3	7.31 ± 0.02	94.0 ± 1.7	47.6 ± 1.6

Mean ± SEM. There were no differences between the groups ($P > 0.05$, ANOVA, $n = 6$ per group).

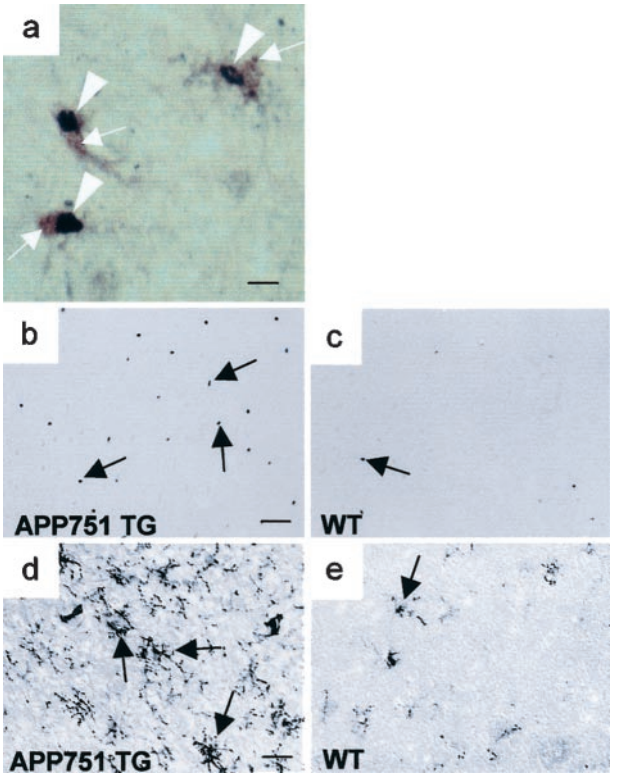

Fig. 3. APP751 TG mice show increased expression of inflammatory markers after 24-h MCA occlusion. (*a*) Double immunohistochemical staining with phospho-p38 MAPK ab (Ni-diaminobenzidine, purple) and F4/80 ab (diaminobenzidine, brown). p38 MAPK activity (arrowheads) is localized to the nuclei of F4/80 positive microglial cells (arrows). (*b*) p38 MAPK activity (arrows) in peri-infarct region of an 8-month-old APP751 TG mouse demonstrated by phospho-p38 MAPK immunohistochemistry. (*c*) An age-matched WT mouse shows only few cells with p38 MAPK activity (arrows) in perifocal cortex. (*d*) F4/80 ab detects robust microgliosis (arrows) in the perifocal cortex of an APP751 mouse. (*e*) Immunoreactivity for F4/80 is much lower in the perifocal cortex of a WT mouse. [Bar = 8 μm (*a*), 100 μm (*b* and *c*), and 50 μm (*d* and *e*)].

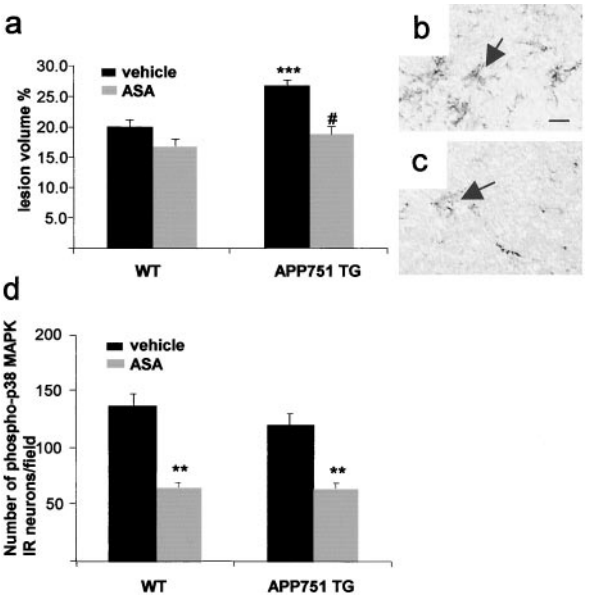

Fig. 4. ASA treatment significantly reduces infarct volume (*a*, # $P < 0.0001$ from vehicle-treated APP751 mice, *t* test) and microgliosis in APP751 TG mice (*b* and *c*). (*a*) ANOVA reveals no difference in lesion volumes between ASA-treated APP751 TG and WT mice but shows larger lesions in vehicle-treated APP751 mice than in any other group (***, $P < 0.001$, ANOVA, $n = 6–8$ mice per group). (*b*) F4/80 positive microglial cells (arrows) in the peri-infarct cortex of a vehicle-treated APP751 TG mouse at 24 h after the MCA occlusion. (*c*) ASA treatment reduces the number of F4/80 positive microglial cells (arrows) in the perifocal cortex of an APP751 mouse. [Scale bar = 15 μm (*b* and *c*)]. (*d*) Expression of phospho-p38 MAPK in ipsilateral cortical neurons at 30 min after the onset of MCA occlusion is reduced by ASA treatment (**, $P < 0.01$, when compared with vehicle-treated mice, *t* test, $n = 3$ mice per group).

difference between the groups. At 24 h, the neuronal induction of phospho-p38 MAPK was completely over in all animals. In contrast, the density of phospho-p38 MAPK-positive microglial cells in peri-infarct regions remained at a significantly higher level in TG mice than in WT mice at 20 months of age (TG: 38 ± 4; WT 9 ± 3 cells; $P < 0.01$, *t* test, $n = 5$ per group) as well as at 8 months (TG: 26 ± 0; WT 6 ± 2 cells; $P < 0.001$, *t* test, $n =$ 3–5) (Fig. 3 *b* and *c*). In line with the difference in p38 MAPK activation, we found enhanced microgliosis (Fig. 3 *d* and *e*) in TG mice compared with WT mice 24 h after ischemia. These findings indicated that inflammation might contribute to the increased vulnerability observed in APP751 TG mice.

Aspirin and Selective p38 MAPK Inhibitor Abolish Increased Inflammation and Ischemic Sensitivity of APP751 TG Mice. ASA is a wide-spectrum antiinflammatory compound known to inhibit activation of various inflammatory enzymes, including cyclooxygenases, iNOS, and even p38 MAPK (41–43). Administration of ASA reduced the infarct volume in APP751 mice to the size indifferent from the infarcts in untreated WT mice but did not significantly alter the infarct size in WT mice (Fig. 4*a*). ASA treatment also reduced microgliosis at 24 h after the onset of MCA occlusion. Although ASA reduced the phospho-p38 MAPK immunoreactivity in the brain as expected, the effect of ASA on the density of phospho-p38 MAPK-positive neurons at 30 min after the onset of MCA occlusion was similar in TG and WT mice (Fig. 4*d*). Importantly, ASA treatment did not alter physiological variables (Table 1) or CBF (data not shown).

To study the specific role of p38 MAPK in the increased ischemic vulnerability of APP751-overexpressing mice, we treated the mice i.p. with SD-282. This compound is a selective and potent inhibitor of p38 α and β with IC_{50} of 1.14 nM and 2.14 μM, respectively. It does not inhibit other MAPKs or related kinases at concentrations under 10 μM. The IC_{50} of SD-282 for lipopolysaccharide-induced tumor necrosis factor α in rat alveolar macrophages is 10 nM. An i.p. injection of 10 mg/kg SD-282 in mice results in 11 μM plasma concentration with a half-life of about 70 min.

When SD-282 was given 10 mg/kg twice with an interval of 2 h, MAPKAP kinase-2 activity in the brains of APP751 mice decreased significantly (−51%, $P < 0.05$, ANOVA, when compared with vehicle-treated APP751 mice) to the level seen in WT mice, in which the treatment with SD-282 did not significantly (−19%) alter the activity (Fig. 5*a*). This result indicates that the inhibitor may sufficiently penetrate the blood–brain barrier to inhibit up-regulated p38 MAPK activity in the brain. Administration of SD-282 reduced the infarct volume by 31% and completely abolished the difference seen between the vehicle-treated TG and WT mice. In addition, a slight reduction (18.7%) was seen also in WT mice (Fig. 5*b*). The SD-282 treatment did not alter CBF (data not shown) or physiological variables (Table 1). Instead, SD-282 reduced microglial activation as we detected a lower number of F4/80-positive ameboid microglial cells in peri-infarct areas at 24 h after the MCA occlusion (WT vehicle treated, 20 ± 1; WT SD-282 treated, 10 ± 3; APP751 TG vehicle treated, 32 ± 5; APP751 TG SD-282 treated, 13 ± 2 cells; $P <$ 0.05, Kruskal–Wallis H test), reduced nuclear binding activity of

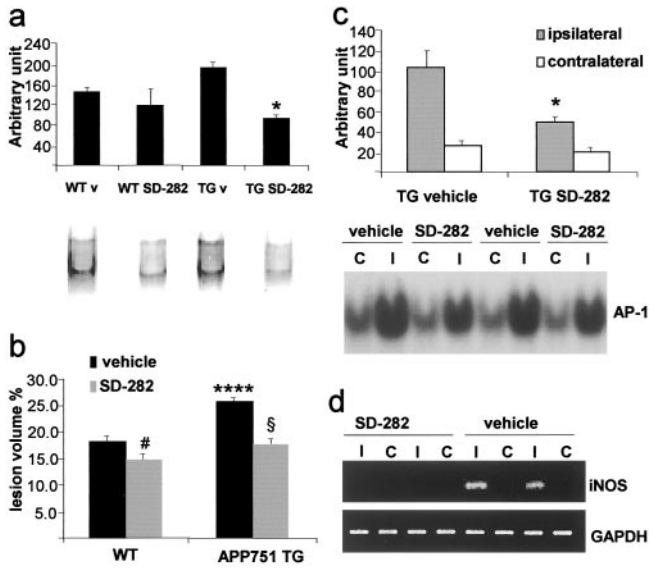

Fig. 5. (*a*) SD-282 treatment significantly reduces MAPKAP kinase-2 activity in cortical homogenates of APP751 TG mice (*, $P < 0.05$, from other groups, ANOVA); v, vehicle. (*b*) SD-282 treatment significantly reduces infarct size in APP751 TG mice (−31%, §, $P < 0.0001$, from vehicle-treated APP751 mice, *t* test) and also slightly (−18.7%, #, $P < 0.05$, *t* test) in WT mice. ANOVA reveals significantly larger lesions in vehicle-treated APP751 TG mice than in other groups (****, $P < 0.0001$). Data were collected from five to six mice per group. (*c*) SD-282 treatment reduces nuclear binding activity of AP-1 in the ipsilateral cortex of APP751 TG mice (*, $P < 0.05$ from ipsilateral cortex of vehicle-treated APP751 mice, *t* test, $n = 4$ mice per group); C, contralateral; I, ipsilateral cortex. (*d*) SD-282 treatment blocks the expression of iNOS mRNA in APP751 TG mice. RT-PCR for glyceraldehyde-3-phosphate dehydrogenase shows equal loading of RNA samples; C, contralateral; I, ipsilateral.

AP-1 (Fig. 5*c*), and reduced iNOS expression (Fig. 5*d*) in APP751 mice after ischemia, indicating amelioration of inflammation and p38 MAPK signaling pathway in the treated mice.

Discussion

We have demonstrated that neuronal overexpression of human wild-type APP751 in mice, which does not result in plaque formation, increases neuronal vulnerability and microgliosis after ischemic insult. p38 MAPK activity is up-regulated specifically in microglial cells of APP751 mice, suggesting that neuronal overexpression of APP751 stimulates microglial cells rendering the brain more vulnerable to ischemia. Consistent with this hypothesis, aspirin, a wide-spectrum antiinflammatory drug with ability to inhibit AP-1 and nuclear factor κB (NF-κB) DNA binding (44), and SD-282, a selective and potent inhibitor of p38 MAPK, abolish both the increased neuronal vulnerability and enhanced inflammation. Even though the F10 pedigree of APP751 TG mice do not develop as severe learning and memory deficit as the F15 mice by 6 months of age (34), both pedigrees showed similar vulnerability to focal ischemic damage at 8 months of age. This suggests that the eventual molecular mechanisms leading to these two kinds of pathologies may be different, as also supported by our finding that ischemic vulnerability did not increase between 8 and 20 months of age unlike the behavioral deficit. Whether anti-inflammatories ameliorate the behavioral deficit in these mice remains to be investigated.

Previous studies have demonstrated that also transgenic mice expressing mutant APP have increased ischemic vulnerability (38), which is in agreement with our findings. Mutant APP mice show Aβ-mediated cerebrovascular dysfunction (38, 45, 46), which may be a mechanism behind the increased cerebral vulnerability observed in those mice. Unlike the mutant APP mice, which produce high Aβ concentrations in the brain, APP751 mice have normal CBF and cerebral vascular reactivity to acetylcholine, excluding the role of impaired vasodilation in the increased vulnerability observed in the present study.

It is well established that p38 MAPK pathway in inflammatory cells activates transcription factors such as NF-κB and AP-1, resulting in the expression of iNOS, tumor necrosis factor-α, and IL-1β (47), all of which have been implicated in ischemic neuronal death. Our finding that attenuation of ischemia-induced expression of iNOS mRNA and AP-1 binding activity is associated with reduced infarct size in APP751 mice after SD-282 treatment supports the hypothesis that reduction of p38 MAPK-mediated inflammation is responsible for the enhanced ischemic vulnerability in APP751 mouse brain.

We found that p38 MAPK is transiently activated in neurons 30 min after the onset of focal ischemia. p38 MAPK activation in neurons was similar in APP751 and WT mice, indicating that this neuronal activation is unlikely to have a role in the increased ischemic vulnerability seen in APP751 mice. However, it is well possible that inhibition of p38 MAPK pathway is beneficial in ischemic injury in general because p38 MAPK activation can promote apoptotic neuronal death (48–50). In agreement with this idea, treatment with the specific p38 MAPK inhibitor resulted in a slight reduction of infarct size in WT mice, a finding previously reported in rat ischemia model (51).

Signaling pathways of several MAPKs, including p38 MAPK, are crucial for leukocyte adhesion to endothelium (47), suggesting that inhibition of p38 MAPK could reduce inflammation and ischemic brain injury by preventing recruitment of leukocytes into the ischemic brain territory. Because previous studies have demonstrated that anti-adhesion therapies are beneficial only in transient ischemia models, which allow reperfusion to the ischemic brain, but not in permanent ischemia model used in the present study (52), it is unlikely that p38 MAPK of endothelial cells or leukocytes has a significant role in the ischemic vulnerability observed in APP751 mice. Moreover, we failed to detect any activated p38 MAPK in the endothelial cells, and the treatment with the specific inhibitor of p38 MAPK did not reduce the number of peripheral cells detected in the ischemic core of APP751 mice (unpublished data).

Similar to sporadic AD cases, our transgenic mouse model overexpresses human wild-type APP751 in neurons, recapitulates early histopathological features of AD, and develops a specific and progressive memory and learning impairment (33–36). Our finding that p38 MAPK mediates ischemic brain vulnerability in APP751-overexpressing mice may have clinical implications. A vast majority of AD patients exhibit cerebrovascular pathology (20). Vascular risk factors also intensify the AD symptoms, and AD pathology is more severe in patients with coexisting cerebral infarcts (22, 23). Because inflammation is thought to contribute to the progression of AD, our demonstration that ischemia-induced inflammation is more detrimental in APP751-overexpressing mice than in WT mice further supports the hypothesis that cerebrovascular diseases enhance AD pathology by a mechanism which may be prevented by antiinflammatory drugs such as p38 MAPK inhibitors.

We are grateful to Dr. Ghislain Opdenakker for helpful suggestions and critical reading of the manuscript. This study was supported by Grant Agency of the Czech Republic Grant 309/00/1656, the Sigrid Juselius Foundation, and the Saastamoinen Foundation, Finland.

1. Price, D. L., Tanzi, R. E., Borchelt, D. R. & Sisodia, S. S. (1998) *Annu. Rev. Genet.* **32,** 461–493.
2. Selkoe, D. J. (2001) *Physiol. Rev.* **81,** 741–766.
3. Farlow, M. R. (1998) *Am. J. Health Syst. Pharm.* **55,** S5–S10.
4. Ray, W. J., Ashall, F. & Goate, A. M. (1998) *Mol. Med. Today* **4,** 151–157.
5. van Leeuwen, F. W. & Hol, E. M. (1999) *J. Neural Transm. Suppl.* **57,** 137–159.

6. Beyreuther, K., Pollwein, P., Multhaup, G., Monning, U., Konig, G., Dyrks, T., Schubert, W. & Masters, C. L. (1993) *Ann. N.Y. Acad. Sci.* **695,** 91–102.
7. McGeer, P. L., Schulzer, M. & McGeer, E. G. (1996) *Neurology* **47,** 425–432.
8. Eikelenboom, P. & Veerhuis, R. (1996) *Neurobiol. Aging* **17,** 673–680.
9. Kalaria, R. (1999) *Curr. Opin. Hematol.* **6,** 15–24.
10. McGeer, P. L. & McGeer, E. G. (1999) *J. Leukocyte Biol.* **65,** 409–415.
11. Akiyama, H., Barger, S., Barnum, S., Bradt, B., Bauer, J., Cole, G. M., Cooper, N. R., Eikelenboom, P., Emmerling, M., Fiebich, B. L., *et al.* (2000) *Neurobiol. Aging* **21,** 383–421.
12. Barger, S. W. & Harmon, A. D. (1997) *Nature (London)* **388,** 878–881.
13. London, J. A., Biegel, D. & Pachter, J. S. (1996) *Proc. Natl. Acad. Sci. USA* **93,** 4147–4152.
14. Meda, L., Cassatella, M. A., Szendrei, G. I., Otvos, L., Jr., Baron, P., Villalba, M., Ferrari, D. & Rossi F. (1995) *Nature (London)* **374,** 647–650.
15. Neve, R. L. & Robakis, N. K. (1998) *Trends Neurosci.* **21,** 15–19.
16. Games, D., Adams, D., Alessandrini, R., Barbour, R., Berthelette, P., Blackwell, C., Carr, T., Clemens, J., Donaldson, T., Gillespie, F., *et al*. (1995) *Nature (London)* **373,** 523–527.
17. Hsiao, K., Chapman, P., Nilsen, S., Eckman, C., Harigaya, Y., Younkin, S., Yang, F. & Cole, G. (1996) *Science* **274,** 99–102.
18. Lamb, B. T., Bardel, K. A., Kulnane, L. S., Anderson, J. J., Holtz, G., Wagner, S. L., Sisodia, S. S. & Hoeger, E. J. (1999) *Nat. Neurosci.* **2,** 695–697.
19. Holcomb, L., Gordon, M. N., McGowan, E., Yu, X., Benkovic, S., Jantzen, P., Wright, K., Saad, I., Mueller, R., Morgan, D., *et al*. (1998) *Nat. Med.* **4,** 97–100.
20. Breteler, M. M. (2000) *Neurobiol. Aging* **21,** 153–160.
21. Kalaria, R. N. (2000) *Neurobiol. Aging* **21,** 321–330.
22. Snowdon, D. A., Greiner, L. H., Mortimer, J. A., Riley, K. P., Greiner, P. A. & Markesbery, W. R. (1997) *JAMA* **277,** 813–817.
23. Nagy, Z., Esiri, M. M., Jobst, K. A., Morris, J. H., King, E. M., McDonald, B., Joachim, C., Litchfield, S., Barnetson, L. & Smith, A. D. (1997) *J. Neuropathol. Exp. Neurol.* **56,** 165–170.
24. Dirnagl, U., Iadecola, C. & Moskowitz, M. A. (1999) *Trends Neurosci.* **22,** 391–397.
25. Barone, F. C. & Feuerstein, G. Z. (1999) *J. Cereb. Blood Flow Metab.* **19,** 819–834.
26. Iadecola, C. & Alexander, M. (2001) *Curr. Opin. Neurol.* **14,** 89–94.
27. del Zoppo, G. J., Becker, K. J. & Hallenbeck, J. M. (2001) *Arch. Neurol.* **58,** 669–672.
28. Yrjanheikki, J., Keinanen, R., Pellikka, M., Hokfelt, T. & Koistinaho, J. (1998) *Proc. Natl. Acad. Sci. USA* **95,** 15769–15774.
29. Yrjanheikki, J., Tikka, T., Keinanen, R., Goldsteins, G., Chan, P. H. & Koistinaho, J. (1999) *Proc. Natl. Acad. Sci. USA* **96,** 13496–13500.
30. del Zoppo, G., Ginis, I., Hallenbeck, J. M., Iadecola, C., Wang, X. & Feuerstein, G. Z. (2000) *Brain Pathol.* **10,** 95–112.
31. Iadecola, C. & Ross, M. E. (1997) *Ann. N.Y. Acad. Sci.* **835,** 203–217.
32. Lim, G. P., Yang, F., Chu, T., Chen, P., Beech, W., Teter, B., Tran, T., Ubeda, O., Ashe, K. H., Frautschy, S. A., *et al*. (2000) *J. Neurosci.* **20,** 5709–5714.
33. Quon, D., Wang, Y., Catalano, R., Scardina, J. M., Murakami, K. & Cordell, B. (1991) *Nature (London)* **352,** 239–241.
34. Koistinaho, M., Ort, M., Cimadevilla, J. M., Vondrous, R., Cordell, B., Koistinaho, J., Bures, J. & Higgins, L. S. (2001) *Proc. Natl. Acad. Sci. USA* **98,** 14675–14680.
35. Higgins, L. S., Rodems, J. M., Catalano, R., Quon, D. & Cordell, B. (1995) *Proc. Natl. Acad. Sci. USA* **92,** 4402–4406.
36. Higgins, L. S., Holtzman, D. M., Rabin J., Mobley, W. C. & Cordell, B. (1994) *Ann. Neurol.* **35,** 598–607.
37. Welsh, F. A., Sakamoto, T., McKee, A. E. & Sims, R. E. (1987) *J. Neurochem.* **49,** 846–851.
38. Zhang, F., Eckman, C., Younkin, S., Hsiao, K. K. & Iadecola, C. (1997) *J. Neurosci.* **17,** 7655–7661.
39. Dignam, J. D., Lebovitz, R. M. & Roeder, R. G. (1983) *Nucleic Acids Res.* **11,** 1475–1489.
40. Helenius, M., Hänninen, M., Lehtinen, S. & Salminen, A. (1996) *J. Mol. Cell Cardiol.* **28,** 487–498.
41. Abramson, S., Korchak, H., Ludewig, R., Edelson, H., Haines, K., Levin, R. I., Herman, R., Rider, L., Kimmel, S. & Weissmann, G. (1985) *Proc. Natl. Acad. Sci. USA* **82,** 7227–7231.
42. Amin, A. R., Vyas, P., Attur, M., Leszczynska-Piziak, J., Patel, I. R., Weissmann, G. & Abramson, S. B. (1995) *Proc. Natl. Acad. Sci. USA* **92,** 7926–7930.
43. Huang, C., Ma, W.-Y., Hanenberger, D., Cleary, M. P., Bowden, T. & Dong, Z. (1997) *J. Biol. Chem.* **272,** 26325–26331.
44. Grilli, M., Pizzi, M., Memo, M. & Spano, P. F. (1996) *Science* **274,** 1383–1385.
45. Niwa, K., Carlson, G. A. & Iadecola, C. (2000) *J. Cereb. Blood Flow Metab.* **20,** 1659–1668.
46. Iadecola, C., Zhang, F., Niwa, K., Eckman, C., Turner, S. K., Fischer, E., Younkin, S., Borchelt, D. R., Hsiao, K. K. & Carlson, G. A. (1999) *Nat. Neurosci.* **2,** 157–161.
47. Herlaar, E. & Brown, Z. (1999) *Mol. Med. Today* **5,** 439–447.
48. Harper, S. J. & LoGrasso, P. (2001) *Cell Signal.* **13,** 299–310.
49. McLaughlin, B., Pal, S., Tran, M. P., Parsons, A. A., Barone, F. C., Erhardt, J. A. & Aizenman, E. (2001) *J. Neurosci.* **21,** 3303–3311.
50. Ciesielski-Treska, J., Ulrich, G., Chasserot-Golaz, S., Zwiller, J., Revel, M. O., Aunis, D. & Bader, M. F. (2001) *J. Biol. Chem.* **276,** 13113–13120.
51. Barone, F. C., Irving, E. A., Ray, A. M., Lee, J. C., Kassis, S., Kumar, S., Badger, A. M., White, R. F., McVey, M. J., Legos, J. J., *et al*. (2001) *J. Pharmacol. Exp. Ther.* **296,** 312–321.
52. Sharkey, J., Kelly, J. S. & Butcher, S. P. (1997) in *Clinical Pharmacology of Cerebral Ischemia*, eds. Ter Horst, G. J. & Korf, J. (Humana, Totowa, NJ), pp. 253–263.